MDPI

Article

Enhanced Methanogenesis of Waste-Activated Sludge (WAS) in a Continuous Stirring Tank Reactor with Stealth Electrodes

Wen He, Dahai Zhang, Lu Zhang, Zhuanyi Ai, Zechong Guo *, Tongyi Yang, Linzhi Zhai and Cheng Huang *

School of Environmental and Chemical Engineering, Jiangsu University of Science and Technology, Zhenjiang 212100, China
* Correspondence: guozechong@just.edu.cn (Z.G.); chenghuang@just.edu.cn (C.H.)

Abstract: The integration of a microbial electrolysis cell (MEC) is an effective strategy for enhancing the efficiency and stability of an anaerobic digestion (AD) system for energy recovery from waste-activated sludge (WAS). Typically, electrodes are arranged as separate components, potentially disrupting mixing and complicating the reactor configuration, posing challenges for the scaling up of AD-MEC coupling systems. In this study, electrodes were introduced into a continuous stirring tank reactor (CSTR) in a "stealth" manner by integrating them with the inner wall and stirring paddle. This electrode arrangement approach was validated through a sequential batch digestion experiment, resulting in a remarkable 1.5-fold increase in cumulative methane production and a shortened lag period compared to the traditional CSTR with a nonconductive inner wall and stirring paddle. Both the conductive materials (CMs) employed in the electrodes and the electrochemical processes equally contributed to the observed enhancement effect of the electrodes by regulating the evolution of the microbial community within the electrode biofilms, with a specific emphasis on the enrichment of methanogens (primarily *Methanobacterium*). This research offers a potential avenue to solve the contradiction between the electrode introduction and the mixing operation in AD-MEC coupling systems and to contribute to its future commercial application.

Keywords: methane production; waste-activated sludge; microbial electrolysis cell; stealth electrodes

1. Introduction

Waste-activated sludge (WAS), a by-product of sewage treatment, poses significant environmental risks due to its substantial production and high concentration of pollutants [1]. Anaerobic digestion (AD) emerges as a crucial technological solution to mitigate the environmental impact of WAS, simultaneously allowing for the recovery of valuable resources. During AD, with the cooperation of diverse anaerobic microbial populations, organic pollutants are converted into biofuels, primarily hydrogen and methane [2], or high value-added products [3,4]. Despite the promising application prospects, the application of AD in WAS treatment is currently challenged by low efficiency, prolonged lag time, and high sensitivity to environment factors [5].

The microbial electrolysis cell (MEC) serves as a versatile platform technology, achieving the transformation and degradation of organic pollutions through various electrochemical reactions driven by a micro voltage [6]. Due to its high compatibility and complementarity with AD, MEC has been recently introduced into AD systems to enhance their efficiency and stability [7]. Compared with sole AD, a general 30% to 200% increase in the methane productivity of WAS was observed in AD-MEC coupling systems with an external voltage of 0.6–1.2 V [8]. In addition, these hybrid systems demonstrated an enhanced tolerance for adverse environmental factors, such as a high organic load rate, NH_3, and salinity toxicity [7,9]. Furthermore, previous studies suggested that MEC can regulate the development and succession of anaerobic microbial communities, contributing to the stability of AD systems by providing additional metabolism pathways [10].

The energy recovery efficiency of AD-MEC coupling systems is significantly affected by the configuration of electrodes, which determines the internal resistance, fluid state, and mass transfer efficiency of the reactor [8]. Most previous studies employed electrodes in parallel (horizontal or vertical) or concentric configuration, as independent units in addition to AD [11,12], and it has been widely attempted to narrow the anode–cathode distance to reduce the internal resistance and increase the current density [13]. Despite its effectiveness in lab-scale experiments, this electrode arrangement strategy presents great challenges for scaling up due to the difficulties in the reactor assembly and maintenance and the interference with solution mixing [14].

As for the substrates with high viscosity and solid content, like WAS, the efficient conversion of biodegradable waste into biogas requires biological, chemical, and physical uniformity within the digester, which can be only fulfilled by thoroughly mixing [15,16]. Proper mixing arrangements can contribute to the reduction in dead zones, the enhanced mass transfer between microbial populations, the reduction in the substrate size, and the separation of gas from the substrate [17,18]. Shaker and magnetic (or mechanical) stirring, located at the bottom of the reactor, are the most common mixing methods in current cases [11,19], which, unfortunately, make it difficult to achieve sufficient mixing of substrates, especially in large-scale devices [18]. Notably, it was recently found that increasing the driving force by mixing improves the proton transfer rate between electrodes with a large distance, and thus reduces the internal resistance [20], which implies that sacrificing mixing for the purpose of shortening electrode spacing may not be inevitable. Therefore, an alternative design for electrode arrangements that meets the mixing needs is required.

A potential solution to the above issue is introducing electrochemical electrodes in a "stealth" manner, i.e., integrating electrochemical electrodes with the original structure of AD reactors (such as the reactor's inner wall and stirring paddle), rather than as separate units. The effectiveness of this strategy in treating high-strength food waste has been demonstrated by the research of Park et al. [21,22], which observed enhanced energy efficiency and systemic stability by employing a bioelectrochemcial anaerobic digestion reactor with a rotating STS304 impeller anode. So far, there are few similar attempts in WAS treatment, and the promoting mechanism of stealth electrodes remains unrevealed, especially the impact of the conductive materials (CM) used in electrodes and electrochemical processes on the development of the microbial community in electrode biofilms and bulk sludge has not been investigated in previous studies, which may play a crucial role in enhancing the efficiency and stability of AD systems.

Therefore, in this study, "stealth" electrodes are introduced into a continuous stirring tank reactor (CSTR) for WAS digestion. Specifically, the carbon felt anode was affixed to the reactor's inner wall, and the cathode was integrated with the stainless-steel stirring paddle (note as AD-MEC). Ordinary CSTRs with nonconductive inner walls and stirring paddles (Group AD) and reactors with conductive inner walls and stirring paddles but without an applied voltage (Group AD-CM) were established as control tests to reveal the effect of conductive materials and electrochemical processes. The methane-producing performance and organic pollutant removal of each group were investigated. Microbial community analysis was performed to reveal the impact of electrochemical intervention on the development of the methanogenic community in biofilm and bulk sludge. In addition, the electrochemical efficiency and energy budget were analyzed to evaluate the contribution of electrochemical processes. The results of this research can offer new technical insights for upgrading AD systems of WAS through the integration of bioelectrochemical technology.

2. Materials and Methods

2.1. Reactor Configuration and Operation

In this study, six reactors were employed and classified into three groups: AD-MEC, AD-CM, and AD, each with two parallel setups. The reactor was made of an organic glass cylinder (10 cm in diameter and a total height of 20 cm) with a working volume of 1 L.

The reactor was outfitted with an electric stirring device, consisting of an electric motor, a controller, and a stirring paddle. The primary differences in structure among the three groups primarily manifested in the configuration of the stirring paddle and the inner wall of the reactor.

In the AD-MEC reactor, the stirring paddle also functioned as an electrochemical cathode, constructed from stainless steel in a flat shape with dimensions of 6 cm × 6 cm. The stirring paddle was connected to the negative pole of a DC power supply through an electric slip ring, which facilitated the transfer of electricity from a stationary structure to a rotating one. The anode, made of carbon felt (31 cm × 15 cm), was affixed to the inner wall of the reactor. A titanium wire traversed the anode, passed over the top, and connected to the positive pole of the power supply. An external voltage was applied between the anode and cathode. An Ag/AgCl reference electrode (0.197 V vs. the standard hydrogen electrode, SHE) was inserted into the reactor for electrode potential measurement. Current in the circuit and electrode potentials were measured using a multimeter/data acquisition system (THMA, Tenghui Instrument, Inc., Ningbo, China). The configuration of the AD-MEC reactor is illustrated in Figure 1. The AD-CM reactor was also equipped with the same stainless stirring paddle and carbon felt as AD-MEC but without the application of an external voltage. In the AD reactor, nonconductive wool felt and a polytetrafluoroethylene stirring paddle of identical dimensions were used as substitutes for the carbon felt and stainless-steel paddle, respectively.
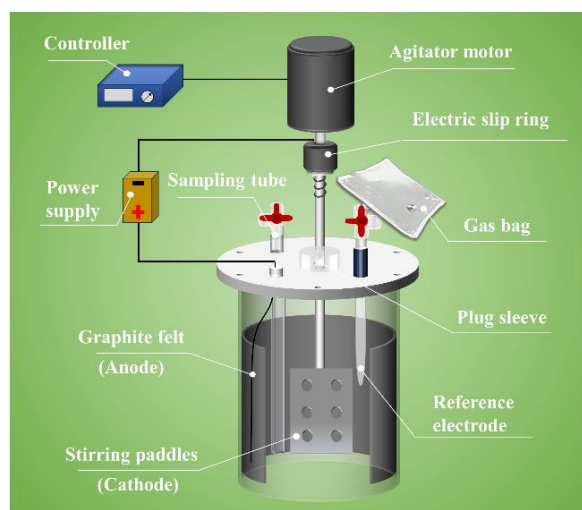

Figure 1. Configuration of AD-MEC reactor.

Prior to formal operation, AD-MEC reactors underwent a batch mode start-up to establish electrochemical functions. Specifically, all reactors were inoculated with a mixture of 50 mL of raw WAS and 950 mL of the culture solution, which contained sodium acetate (1000 mg/L), a 50 mmol phosphate buffer solution (PBS), and trace elements [10]. The culture solution was refreshed every two days until stable current outputs were obtained, and anode potentials dropped below −400 mV in AD-MEC, indicating the successful acclimation of electrodes. Subsequently, the culture solution was replaced with alkaline-pretreated sludge, and the recording of the running time commenced. All reactors were continuously stirred at a rate of 80 rpm and operated at room temperature. AD-MEC reactors were provided with a 0.8 V external voltage. In the tests for electrochemical efficiency analysis, another two AD-MEC reactors with voltages of 0.6 V and 1.0 V were conducted under the same conditions. The gas produced by each reactor was collected using an aluminum gas bag. Sludge and gas samples were collected every day for analysis.

2.2. WAS Characteristics and Pretreatment

The WAS used in this study was obtained from the secondary sedimentation tank in the Jingkou Wastewater Treatment Plant (Zhenjiang, China). After a 24 h settling period, the supernatant was removed, and the concentrated sludge underwent screening with a 40-mesh sieve to remove impurities. To enhance the release of intracellular organic matter in WAS, an alkaline pretreatment was conducted by adjusting the pH of WAS to 10.0 with 10 mol/L NaOH solution. The main properties of the pretreated sludge were as follows: total suspended solids (TSS) 21.6 g/L, volatile suspended solids (VSS) 14.8 g/L, total chemical oxygen demand (TCOD) 17,199.0 mg/L, soluble chemical oxygen demand (SCOD) 2851.8 mg/L, soluble carbohydrate 182.7 mg/L, soluble protein 56.2 mg/L, and total volatile fatty acids (VFAs) 652.5 mg/L.

2.3. Analytical Methods

The biogas composition (H_2, CO_2, and CH_4) was analyzed using a gas chromatograph (GC-9790II, Fuli Analytical Instruments Inc., Zhejiang, China) equipped with a thermal conductivity detector, following procedures outlined in the literature [23]. Total suspended solids (TSS) and volatile suspended solids (VSS) were determined by the constant weight method at 105 °C and 600 °C, respectively. TCOD was measured using the national standard method. Before determining the soluble components (SCOD, total soluble carbohydrate, total soluble protein, and VFAs), the sludge samples were centrifuged at 8000 rpm and filtered with a 0.45 μm filter. Soluble carbohydrate was determined by the phenol-sulfuric acid method. Soluble protein was determined using a BCA protein kit method (Sangon Biotech, Shanghai, China). VFAs (acetic acid, propionic acid, butyric acid, and valeric acid) were determined by gas chromatography (7890 A, Agilent Technologies (China) Co., Ltd., Shanghai, China), equipped with a flame ionization detector, as described in a previous study [23].

2.4. Biomass Sampling and Analysis

After operation, the bulk sludge and biofilms that adhered to the carbon felt (or wool felt) were collected. The sampling method of the biofilm was as follows: carbon felt (or wool felt) was taken out from the reactor after operation and washed with sterilized phosphate buffered solution to remove all the biomass. All wash water was collected together and centrifuged at 8000 rpm for 10 min, the supernatant was removed, and the precipitate was stored at −20 °C for microbial structure analysis. The sample DNA was extracted using a DNA extraction kit (Omega Bio-Tek D55625, Norcross, GA, USA). 16Sr DNA sequencing was performed by Majorbio Co., Ltd. (Shanghai, China), with general primers 515F (50-GTGCCAGCMGCCGCGG-30) and 806R (50-GGACTACHVG GGTWTCTAAT-30). The microbial diversity index and OTUs were determined for each sample, and hierarchical clustering analysis was calculated by I-Sanger online data processing, developed by Majorbio.

2.5. Calculations

The kinetic parameters of methane production were obtained by fitting the cumulative methane production curve with the Gompertz equation (Equation (1)).

$$P_{(t)} = P_m \cdot exp\left\{ -exp\left[\frac{R_m \cdot e}{P_m}(\lambda - t) + 1 \right] \right\} \tag{1}$$

where $P_{(t)}$ represents the cumulative CH_4 production (mL/g VSS); P_m is the maximum potential for methane generation (mL/g VSS); R_m represents the peak CH_4 production rate (mL/(gVSS·d)); λ is the duration of the lag phase (d); and e is a constant with a value of 2.72.

The electrochemical efficiency was calculated according to the literature [24]. The significance of the results was determined through analyses of variance (ANOVAs) at a significance level of 0.05.

3. Results and Discussion

3.1. Substrate Conversion Performance

Methane production efficiency is intricately linked to the effective removal of organic matter from the substrate. In this study, it was observed that the introduction of electrodes in a "stealth" manner resulted in a more efficient substrate conversion. In comparison to AD, AD-MEC exhibited a notable enhancement in the removal of TSS, VSS, and TCOD (Figure 2a), increased by 56.0%, 46.7%, and 34.6%, respectively. The organic matter removal in AD-CM falls between AD and AD-MEC, with increases of 18.6%, 16.6%, and 8.6%, respectively, compared to AD. This indicates that the promoting effect of electrodes on organic substrate conversion partially arises from the CMs used in electrodes and, to a greater extent, from the electrochemical processes driven by external voltages.
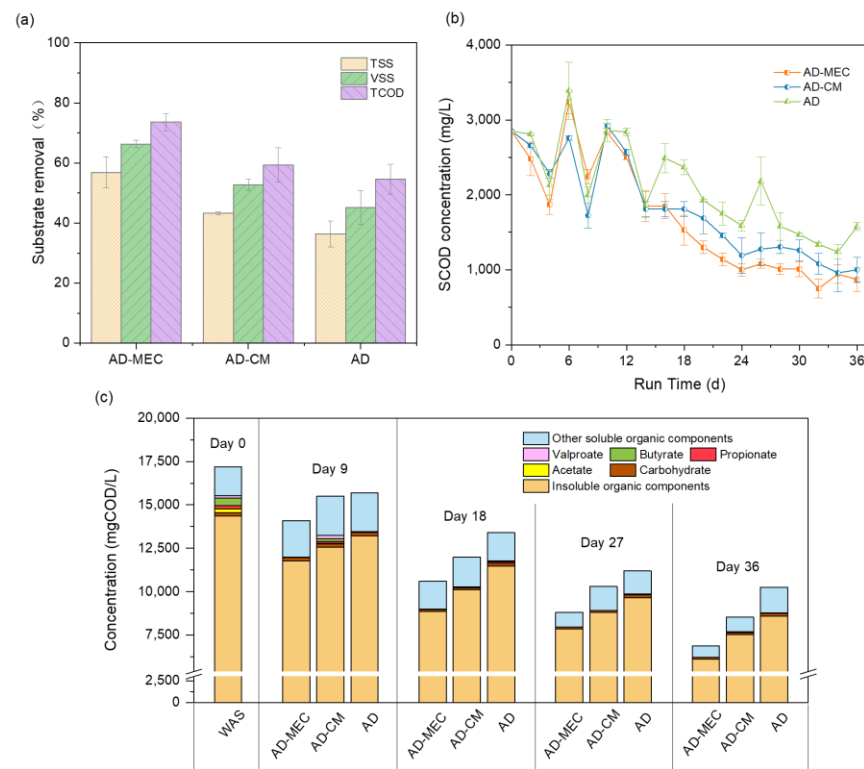

Figure 2. Overall substrate removal (**a**), SCOD concentration variation over time (**b**), and organic substrate composition at different time points (Day 0, 9, 18, 27, and 36) (**c**).

The trends in the SCOD concentration for each group over time were generally consistent, displaying significant fluctuations in the early stage and a gradual decrease after 12 days (Figure 2b). The SCOD content was influenced by both methanogenic consumption and solid substrate hydrolysis. The early increase, as observed in previous studies, was associated with the leaching of organic matter from WAS cells or extracellular polymeric substances (EPS) [25]. In the later stage, due to accelerated methanogenesis, the consumption rate of soluble organic matter exceeded its generation rate, resulting in a decrease in SCOD concentration. At this stage, the SCOD concentrations of the three groups showed significant differences ($p < 0.05$), with AD being the highest, followed by AD-CM, while AD-MEC was the lowest, indicating that the introduction of electrodes accelerated the conversion of the substrate.

To elucidate the impact of electrodes on the conversion of organic substrates, an organic composition analysis (based on a COD equivalent calculation) was conducted with the data at different time points (Day 0, 9, 18, 27, and 36) (Figure 2c). Among the soluble organic components, the content of fermentation products, such as VFAs, was relatively low. Similar to previous cases [11,23], VFA concentrations decreased with the

implementation of anaerobic fermentation. Particularly in the AD-MEC group, VFAs were almost completely depleted in the late stage. In all groups, insoluble organic compounds dominated throughout the entire digestion period, accounting for 80% to 90% of the total organic matter. They gradually decomposed and were converted to methane by anaerobic microorganisms during fermentation. At each time point, the concentration of insoluble components in AD, AD-CM, and AD-MEC decreased sequentially. After fermentation, 40.1% of the insoluble organic matter in AD was removed, a similar level to that reported in the literature [26], whereas in AD-MEC, the removal rate increased to 57.4%, suggesting the promoting effect of electrodes on substrate hydrolysis.

3.2. Methanogenic Performance

Throughout the entire AD period, the daily methane production in all groups exhibited a trend of an initial increase followed by a decline (Figure 3a), suggesting a sufficient recovery of the methane potential. Despite a relatively large standard deviation between parallel samples, the differences among the three groups still remained statistically significant ($p < 0.05$). During the operational process, the AD control consistently maintained a low level of methane production (averaging less than 2 mL/gVSS). In comparison, the methane production of AD-CM generally increased in the initial 28 days, with a peak production of 10.1 mL/gVSS on Day 29, and then showed a downward trend. In contrast, in AD-MEC, following the early fluctuation, the methane production exhibited a rapid increase from Day 12 to Day 20, reaching its peak on Day 21 at 14.0 mL/gVSS, and it gradually declined thereafter. The shift in the peak time of the daily methane production suggests that the introduction of the electrochemical process shortened the lag period of the methanogenic population.
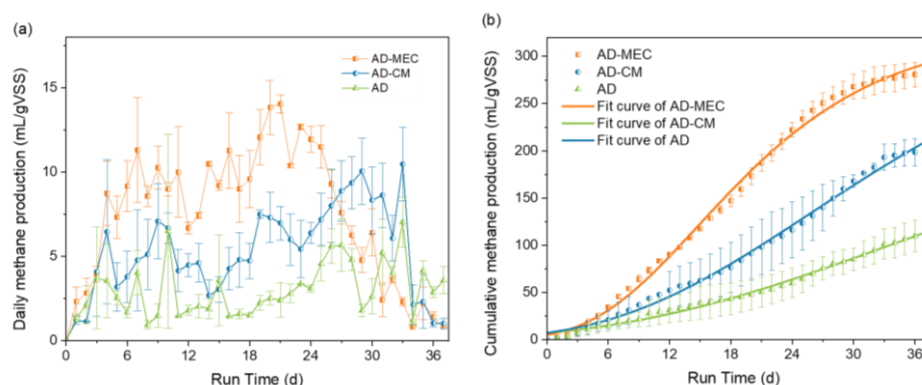

Figure 3. Daily methane production (**a**) and cumulative methane production (**b**).

Compared to the AD control group, AD-CM exhibited a significant improvement ($p < 0.05$) in cumulative methane production (Figure 3b), rising from a total methane production of 113.1 to 199.6 mL/gVSS. This indicates that the introduction of CMs positively influenced the methanogenic process, aligning with findings from prior studies [27]. Importantly, the cumulative methane production of AD-MEC, reaching 281.6 mL/gVSS, surpassed both AD and AD-CM ($p < 0.05$). This demonstrates that the electrochemical reactions occurring at the cathode and anode, driven by external voltage, had a substantial enhancing effect on the methane production from WAS. In some prior cases, the absence of control experiments has posed challenges in determining whether enhancements should be ascribed to the CMs used in the electrodes or the electrochemical processes. In this study, it can be inferred that both conductive materials and electrochemical processes contributed approximately 50% each to the promotional effect of the electrodes.

The kinetic parameters of methane production processes for the three groups were determined by fitting cumulative production curves using the Gompertz model (Figure 3b and Table 1). The maximum methane production potential (P_m) of AD-MEC was comparable to that of AD-CM, far surpassing that of AD. The maximum methane production

rate (R_m) of AD was the lowest, with only 3.9 mL/(gVSS d), while AD-CM increased by 92%, and AD-MEC increased by 2.0 times compared to AD. The duration of the lag phase exhibited the opposite trend, with AD-MEC being shorter than AD-CM, and AD having the longest lag time. This indicates that the introduction of CMs increased methanogenesis rates and shortened the lag periods, and applying an external voltage on this basis can further enhance the promoting effect.

Table 1. Kinetic parameters estimated by fitting a modified Gompertz model.

Group	Actual Cumulative Production (mL/gVSS)	Kinetic Parameters			
		P_m (mL/gVSS)	R_m (mL/(gVSS·d))	λ (d)	R^2
AD-MEC	281.6 ± 12.9	327.9 ± 6.6	11.7 ± 0.01	4.5 ± 0.3	0.996
AD-CM	199.6 ± 14.0	359.3 ± 28.9	7.1 ± 0.04	6.9 ± 0.4	0.994
AD	113.1 ± 15.7	280.9 ± 46.9	3.9 ± 0.07	8.0 ± 1.4	0.991

In summary, the incorporation of the "stealth" electrodes effectively boosted methanogenic efficiency, leading to a 1.5-fold increase in total methane production compared to the traditional AD system. Half of this improvement is attributed to the introduction of CMs, while the remaining half resulted from the direct or indirect contributions of electrochemical processes. Apart from the rise in total methane production, the electrodes also notably expedited the methane production process and shortened the lag period.

Organic component analysis suggests that, in the WAS digestion process (especially in the later stage), the limiting step was the hydrolysis of solid organic matter rather than methanogenesis. CMs and electrochemistry primarily accelerate the methanogenic process, but their promoting effect on hydrolysis was limited. This limitation may lead to unsatisfactory performance in AD-MEC coupling systems, highlighting the importance of strengthening sludge hydrolysis for fully harnessing the promotional effect of electrochemical units in coupling systems.

While often overlooked, agitation is crucial for enhancing the hydrolysis of sludge throughout the entire digestion process. Generally, the more complex the internal structure of a reactor, the less favorable it is for effective mixing. Therefore, introducing electrodes in a stealthy way can be beneficial in avoiding disruption to the flow state and strengthening sludge hydrolysis. Additionally, the simplified configuration allows for straightforward upgrades through simple modifications to traditional CSTR configurations.

3.3. Microbial Community Structure

To elucidate the electrode's promotion mechanism, both bulk sludge and biofilms adhering to the felt (wool felt in AD and carbon felt in AD-CM and AD-MEC) were collected and subjected to high-throughput sequencing after digestion. Notably, due to the smooth surface and continuous rotation of stirring paddles, which are unfavorable for microbial attachment, no biofilm samples from these surfaces were successfully collected.

According to sequencing analysis, electrodes, CMs, and even the nonconductive carriers significantly influence the microbial community diversity and composition structure (Table 2 and Figure 4). Firstly, the α-diversity of bulk sludge in each group was generally higher than that of biofilms, indicating a screening effect of carriers on attached microorganisms. For instance, the ACE index of bulk sludge after digestion ranged from 1762.7 to 2126.4, whereas the index of biofilm was only from 1425.8 to 1681.5. Similar conclusions can also be drawn from other indices, such as Chao, Shannon, and Simpson. Among the three groups, the diversity of the bulk sludge in AD-MEC was higher than that of AD-CM and AD. Conversely, for the biofilms, AD had the highest diversity, followed by AD-CM, and the lowest was found in AD-MEC. This suggests that the application of CMs and anodic electrochemical reactions further enhanced the screening effect of the carriers.

Table 2. Microbial community α-diversity indexes.

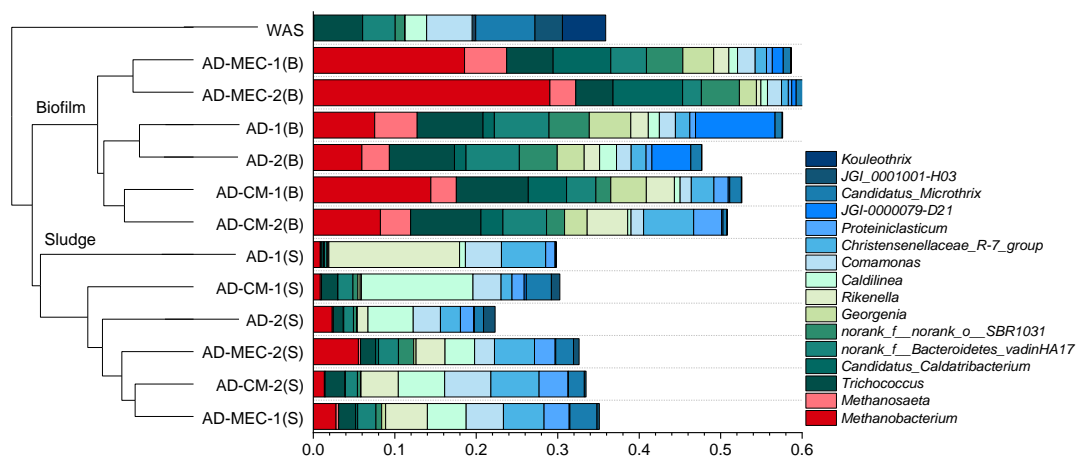| Samples		ACE	Chao	Shannon	Simpson
Initial WAS		1569.2	1563.8	5.35	0.016
Sludge	AD-MEC	2126.4 ± 3.1	2091.8 ± 7.3	5.54 ± 0.08	0.011 ± 0.001
	AD-CM	1941.0 ± 123.8	1922.2 ± 111.5	5.53 ± 0.04	0.010 ± 0.001
	AD	1762.7 ± 232.1	1786.5 ± 213.7	5.27 ± 0.49	0.021 ± 0.014
Biofilm	AD-MEC	1425.8 ± 27.1	1402.6 ± 26.8	4.18 ± 0.29	0.066 ± 0.035
	AD-CM	1600.2 ± 44.5	1579.9 ± 37.5	4.50 ± 0.21	0.040 ± 0.012
	AD	1681.5 ± 27.4	1662.3 ± 51.4	4.66 ± 0.11	0.032 ± 0.008

Figure 4. Bray–Curtis analysis and genera distribution. B stands for biofilm, and S stands for sludge.

According to the Bray–Curtis analysis (Figure 4), a noticeable shift in microbial community structure occurred between the initial WAS, the bulk sludge post-digestion, and the biofilms, and significant differences were observed between the latter two. It was previously reported that MEC electrodes could enhance the presence of bioelectrochemically active microorganisms in the bulk solution and their electron utilization [28]. In this study, however, the community of bulk sludge in the three groups exhibited no significant differences, indicating that the impact of electrodes (or CMs) on microbial community evolution of bulk sludge was relatively low, and the community succession in bulk sludge was not the key reason for the improvement of methanogenic efficiency.

The structure of biofilm communities, in contrast, showed pronounced differentiation under the influence of conductive carriers and electrochemical reactions. From the perspective of genera distribution, the most noteworthy aspect is the variation in the content of methanogens. Firstly, the content of methanogens in the initial WAS were extremely low; however, after digestion, both the biofilm and bulk sludge in each group contained considerable methanogens. Secondly, the presence of carriers was beneficial for the enrichment of methanogens. Even the biofilm of the AD control group (the lowest in biofilm, accounting for about 10% of the total genera) contained more methanogens than the bulk sludge in AD-MEC (the highest in sludge, about 6%). Thirdly, CMs and external voltage significantly increased the content of methanogens in biofilm, which was 9.4~12.7% in AD, 11.9~17.6% in AD-CM, and further increased to 23.8~32.2% in AD-MEC. In this experiment, the detected methanogens mainly consist of two genera, *Methanosaeta* and *Methanobacterium*, with the latter dominating in both biofilm and bulk sludge (more than 59% of methanogens in biofilm and 87% in bulk sludge). *Methanosaeta* could reduce CO_2 to CH_4 with the electrons from syntrophic bacteria or electroactive bacteria [29], playing essential roles in acetophilic methanogenesis. *Methanobacterium*, in contrast, is a typical hydrogenotrophic methanogen with the ability to participate in DIET-type methanogenesis, which was previously reported to be enriched in anaerobic systems with the amendment of CMs or electrodes [30].

Similar to methanogens, there were also significant differences in the bacterial genera distribution between the initial WAS, biofilms, and bulk sludge, while electrodes (or CMs) showed no significant impact on the distribution of biofilm and bulk sludge communities. In the initial WAS, several anaerobic fermentative genera, including *Candidatus_ Microthrix*, *Trichococcus*, *Comamonas*, *Kouleothrix*, and *JGI_0001001-H03* [31–35], dominated the bacterial community, with other genera less than 3%. After digestion, on the contrary, acid-producing bacteria *Caldilinea*, *Comamonas*, *Christensenellaceae_R-7_group*, and *Rikenella* [36–38] became the dominant genera in the bulk sludge. In biofilms, *Trichococcus*, which produces lactate, acetate, formate, ethanol, CO_2, and small amounts of hydrogen under anaerobic conditions [32], was the most abundant, with a relative content ranging from 4.6% to 8.8%. Several other fermentative bacteria, including *Candidatus_Caldatribacterium*, *norank_f_norank_o_SBR1031*, *Georgenia*, and *norank_f_Bacteroidetes _vadinHA17* [39,40], also had a relatively high content in biofilms. The enrichment of these genera provided abundant substrates for methanogens.

In summary, the introduction of electrodes and CMs showed limited effects on the shift of microbial community in bulk sludge but effectively regulated the evolution of the community in biofilms that adhered to their surfaces. CMs induced the enrichment of electroactive methanogens, mainly *Methanobacterium* and *Methanosaeta*, and the presence of electrochemical reactions further strengthened this enriching effect. This explains the improvement in methane production by introducing electrodes.

### 3.4. Electrochemical Efficiency and Energy Budget Analysis

To determine the effect of electrochemical efficiency on the methanogenesis of WAS in AD-MEC systems with stealth electrodes, besides the AD-MEC group with a voltage of 0.8 V, two additional AD-MEC groups with external voltages of 0.6 V and 1.0 V were also conducted under the same condition, and their electrochemical efficiency and methane production capacity were evaluated.

Under all voltage conditions, AD-MEC systems exhibited extremely low electrochemical efficiencies, with an average current of about 1 mV and an anode coulombic efficiency of only 3% (Table 3). This indicates that the electrochemical process influenced methanogenesis mainly by the modulation of the functional microbial community, instead of making a direct contribution. From the perspective of converting organic substrates into methane, the group with a 0.8 V voltage exhibited the best performance, followed by 0.6 V, while under the voltage of 1.0 V, both accumulative methane production and VSS removal significantly decreased. The decline in methanogenic efficiency under a high external voltage may be related to the unfavorable anode potential. The cathode potentials under three voltages were quite similar, maintained around −1.1 V, while the anode potential showed significant differences. The suitable oxidation-reduction potential of methanogens is below −300 mV, especially during the initial cultivation stage. The anode potentials of the 0.6 V and 0.8 V groups were within a suitable range, while the anode potential under 1.0 V rose to −0.16 V, which was unfavorable for the growth and metabolism of methanogens. Based on the electrochemical efficiency and methanogenic performance under different voltages, it can be inferred that, in spite of the unsatisfactory electrochemical performance of the stealth electrodes' arrangement, significant promoting effects can still be achieved by forming a biofilm rich in methanogens due to the adapted habitat created by the electrodes.

Table 3. Electrochemical efficiency under different voltages.

Voltage	External Voltage		
	0.6 V	**0.8 V**	**1.0 V**
Accumulative methane production (mL/gVSS)	240.9	281.6	105.6
VSS removal (%)	52.5	66.3	43.3
Average current (mA)	0.88	1.15	0.85
Average anode potential (V)	−0.53	−0.31	−0.16
Average cathode potential (V)	−1.12	−1.11	−1.16
Coulombic efficiency (%)	3.0	3.1	3.5

The introduction of electrochemical processes has demonstrated various positive effects on anaerobic digestion. However, the incorporation of these processes necessitates a certain level of external energy consumption, and it may be economically unfavorable if the gained energy is insufficient to offset the additional energy cost. According to the energy budget analysis (Figure 5), the energy cost of AD-MEC was actually quite small due to the low current level, which was far less than their energy income. Compared to AD-CM, the AD-MEC groups with external voltages of 0.6 V and 0.8 V achieved positive energy gains. However, under the voltage of 1.0 V, the energy gain was even lower than that of the AD control group. Therefore, it can be concluded that it is economically feasible to introduce the stealth electrodes under the premise of applying appropriate voltage levels (from 0.6 V to 0.8 V in this study).
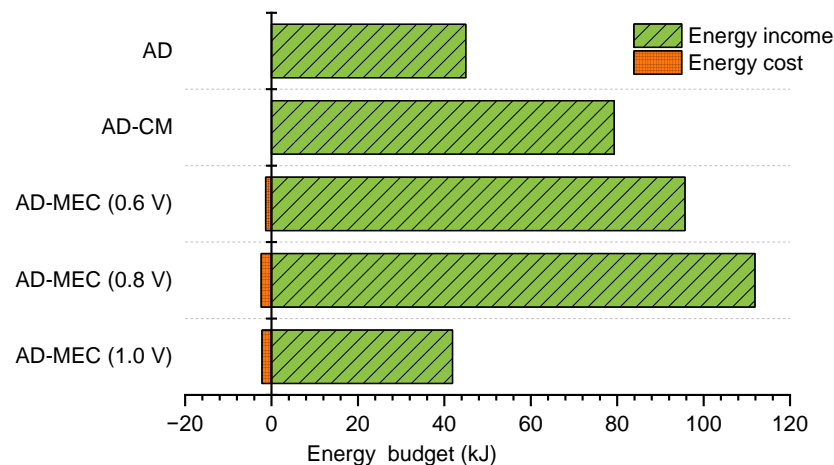
Figure 5. Energy budget analysis.

4. Conclusions

Compared to the traditional CSTR setup, introducing MEC electrodes in a stealth manner, by integrating them with the reactor's inner wall and stirring paddle, significantly enhanced the methanogenic performance, resulting in a 1.5-fold increase in cumulative methane production and a shortened lag period (from 8.0 d to 4.5 d). Both the CMs and the electrochemical reactions contributed equally to the improvement effect of stealth electrodes. CMs facilitated the enrichment of methanogens, particularly, *Methanobacterium* —a hydrogenotrophic methanogen—adhered to the electrode surface within the biofilm, while electrochemical processes further enhanced this enrichment effect by providing a suitable habitat with a low potential. The domestication of electrode biofilms with high methanogenic activity, rather than electrochemical efficiency, played a crucial role in promoting methane production performance in this system. Considering its simplified

configuration and effectiveness in promoting methanogenesis, integrating stealth electrodes represents a potential technical approach for scaling up AD-MEC coupling systems.

Institutional Review Board Statement: Not applicable.

Informed Consent Statement: Not applicable.

Data Availability Statement: Data are contained within the article.

Conflicts of Interest: The authors declare no conflicts of interest.

References

1. Fernández-Fernández, V.; Ramil, M.; Rodríguez, I. Basic micro-pollutants in sludge from municipal wastewater treatment plants in the Northwest Spain: Occurrence and risk assessment of sludge disposal. *Chemosphere* **2023**, *335*, 139094. [CrossRef] [PubMed]
2. Deena, S.R.; Vickram, A.S.; Manikandan, S.; Subbaiya, R.; Karmegam, N.; Ravindran, B.; Chang, S.W.; Awasthi, M.K. Enhanced biogas production from food waste and activated sludge using advanced techniques—A review. *Bioresour. Technol.* **2022**, *355*, 127234. [CrossRef] [PubMed]
3. Núñez, D.; Oulego, P.; Collado, S.; Riera, F.A.; Díaz, M. Separation and purification techniques for the recovery of added-value biocompounds from waste activated sludge. A review. *Resour. Conserv. Recycl.* **2022**, *182*, 106327. [CrossRef]
4. Awasthi, M.K.; Ganeshan, P.; Gohil, N.; Kumar, V.; Singh, V.; Rajendran, K.; Harirchi, S.; Solanki, M.K.; Sindhu, R.; Binod, P.; et al. Advanced approaches for resource recovery from wastewater and activated sludge: A review. *Bioresour. Technol.* **2023**, *384*, 129250. [CrossRef] [PubMed]
5. Luo, J.; Zhang, Q.; Zhao, J.; Wu, Y.; Wu, L.; Li, H.; Tang, M.; Sun, Y.; Guo, W.; Feng, Q.; et al. Potential influences of exogenous pollutants occurred in waste activated sludge on anaerobic digestion: A review. *J. Hazard. Mater.* **2020**, *383*, 121176. [CrossRef] [PubMed]
6. Kadier, A.; Simayi, Y.; Abdeshahian, P.; Azman, N.F.; Chandrasekhar, K.; Kalil, M.S. A comprehensive review of microbial electrolysis cells (MEC) reactor designs and configurations for sustainable hydrogen gas production. *Alex. Eng. J.* **2016**, *55*, 427–443. [CrossRef]
7. Huang, Q.; Liu, Y.; Dhar, B.R. A critical review of microbial electrolysis cells coupled with anaerobic digester for enhanced biomethane recovery from high-strength feedstocks. *Crit. Rev. Environ. Sci. Technol.* **2020**, *52*, 50–89. [CrossRef]
8. Wang, X.-T.; Zhang, Y.-F.; Wang, B.; Wang, S.; Xing, X.; Xu, X.-J.; Liu, W.-Z.; Ren, N.-Q.; Lee, D.-J.; Chen, C. Enhancement of methane production from waste activated sludge using hybrid microbial electrolysis cells-anaerobic digestion (MEC-AD) process—A review. *Bioresour. Technol.* **2022**, *346*, 126641. [CrossRef]
9. De Vrieze, J.; Arends, J.B.A.; Verbeeck, K.; Gildemyn, S.; Rabaey, K. Interfacing anaerobic digestion with (bio)electrochemical systems: Potentials and challenges. *Water Res.* **2018**, *146*, 244–255. [CrossRef]
10. Guo, Z.; Liu, W.; Yang, C.; Gao, L.; Thangavel, S.; Wang, L.; He, Z.; Cai, W.; Wang, A. Computational and experimental analysis of organic degradation positively regulated by bioelectrochemistry in an anaerobic bioreactor system. *Water Res.* **2017**, *125*, 170–179. [CrossRef]
11. Xu, X.-J.; Wang, W.-Q.; Chen, C.; Xie, P.; Liu, W.-Z.; Zhou, X.; Wang, X.-T.; Yuan, Y.; Wang, A.-J.; Lee, D.-J.; et al. Bioelectrochemical system for the enhancement of methane production by anaerobic digestion of alkaline pretreated sludge. *Bioresour. Technol.* **2020**, *304*, 123000. [CrossRef] [PubMed]
12. Hou, Y.; Zhang, R.; Luo, H.; Liu, G.; Kim, Y.; Yu, S.; Zeng, J. Microbial electrolysis cell with spiral wound electrode for wastewater treatment and methane production. *Process Biochem.* **2015**, *50*, 1103–1109. [CrossRef]
13. Im, S.; Ahn, Y.; Chung, J.W. Influence of Electrode Spacing on Methane Production in Microbial Electrolysis Cell Fed with Sewage Sludge. *J. Korean Soc. Environ. Eng.* **2015**, *37*, 682–688. [CrossRef]
14. Park, J.-G.; Jiang, D.; Lee, B.; Jun, H.-B. Towards the practical application of bioelectrochemical anaerobic digestion (BEAD): Insights into electrode materials, reactor configurations, and process designs. *Water Res.* **2020**, *184*, 116214. [CrossRef] [PubMed]
15. Singh, B.; Szamosi, Z.; Siménfalvi, Z. State of the art on mixing in an anaerobic digester: A review. *Renew. Energy* **2019**, *141*, 922–936. [CrossRef]
16. Kaparaju, P.; Buendia, I.; Ellegaard, L.; Angelidakia, I. Effects of mixing on methane production during thermophilic anaerobic digestion of manure: Lab-scale and pilot-scale studies. *Bioresour. Technol.* **2008**, *99*, 4919–4928. [CrossRef] [PubMed]

17. Bridgeman, J. Computational fluid dynamics modelling of sewage sludge mixing in an anaerobic digester. *Adv. Eng. Softw.* **2012**, *44*, 54–62. [CrossRef]

18. Hu, Y.; Zheng, X.; Zhang, S.; Ye, W.; Wu, J.; Poncin, S.; Li, H.Z. Investigation of hydrodynamics in high solid anaerobic digestion by particle image velocimetry and computational fluid dynamics: Role of mixing on flow field and dead zone reduction. *Bioresour. Technol.* **2021**, *319*, 124130. [CrossRef]

19. Yang, C.-X.; Wang, L.; Zhong, Y.-J.; Guo, Z.-C.; Liu, J.; Yu, S.-P.; Sangeetha, T.; Liu, B.-L.; Ni, C.; Guo, H. Efficient methane production from waste activated sludge and Fenton-like pretreated rice straw in an integrated bio-electrochemical system. *Sci. Total Environ.* **2022**, *813*, 152411. [CrossRef]

20. Park, J.-G.; Lee, B.; Shi, P.; Kim, Y.; Jun, H.-B. Effects of electrode distance and mixing velocity on current density and methane production in an anaerobic digester equipped with a microbial methanogenesis cell. *Int. J. Hydrogen Energy* **2017**, *42*, 27732–27740. [CrossRef]

21. Park, J.; Lee, B.; Shin, W.; Jo, S.; Jun, H. Psychrophilic methanogenesis of food waste in a bio-electrochemical anaerobic digester with rotating impeller electrode. *J. Clean. Prod.* **2018**, *188*, 556–567. [CrossRef]

22. Park, J.; Lee, B.; Shin, W.; Jo, S.; Jun, H. Application of a rotating impeller anode in a bioelectrochemical anaerobic digestion reactor for methane production from high-strength food waste. *Bioresour. Technol.* **2018**, *259*, 423–432. [CrossRef] [PubMed]

23. Wang, L.; Liu, C.; Fan, X.; Yang, C.; Zhou, X.; Guo, Z. Methane Promotion of Waste Sludge Anaerobic Digestion: Effect of Typical Metal Meshes on Community Evolution and Electron Transfer. *Water* **2022**, *14*, 3129. [CrossRef]

24. Guo, Z.; Thangavel, S.; Wang, L.; He, Z.; Cai, W.; Wang, A.; Liu, W. Efficient Methane Production from Beer Wastewater in a Membraneless Microbial Electrolysis Cell with a Stacked Cathode: The Effect of the Cathode/Anode Ratio on Bioenergy Recovery. *Energy Fuels* **2016**, *31*, 615–620. [CrossRef]

25. Pasalari, H.; Esrafili, A.; Rezaee, A.; Gholami, M.; Farzadkia, M. Electrochemical oxidation pretreatment for enhanced methane potential from landfill leachate in anaerobic co-digestion process: Performance, Gompertz model, and energy assessment. *Chem. Eng. J.* **2021**, *422*, 130046. [CrossRef]

26. Feng, Y.; Zhang, Y.; Chen, S.; Quan, X. Enhanced production of methane from waste activated sludge by the combination of high-solid anaerobic digestion and microbial electrolysis cell with iron–graphite electrode. *Chem. Eng. J.* **2015**, *259*, 787–794. [CrossRef]

27. Liang, J.; Luo, L.; Wong, J.W.C.; He, D. Recent advances in conductive materials amended anaerobic co-digestion of food waste and municipal organic solid waste: Roles, mechanisms, and potential application. *Bioresour. Technol.* **2022**, *360*, 127613. [CrossRef]

28. Cai, W.; Liu, W.; Yang, C.; Wang, L.; Liang, B.; Thangavel, S.; Guo, Z.; Wang, A. Biocathodic Methanogenic Community in an Integrated Anaerobic Digestion and Microbial Electrolysis System for Enhancement of Methane Production from Waste Sludge. *ACS Sustain. Chem. Eng.* **2016**, *4*, 4913–4921. [CrossRef]

29. Rotaru, A.E.; Shrestha, P.M.; Liu, F.; Shrestha, M.; Shrestha, D.; Embree, M.; Zengler, K.; Wardman, C.; Nevin, K.P.; Lovley, D.R. A new model for electron flow during anaerobic digestion: Direct interspecies electron transfer to Methanosaeta for the reduction of carbon dioxide to methane. *Energy Environ. Sci.* **2013**, *7*, 408–415. [CrossRef]

30. Zheng, S.; Liu, F.; Wang, B.; Zhang, Y.; Lovley, D.R. Methanobacterium Capable of Direct Interspecies Electron Transfer. *Environ. Sci. Technol.* **2020**, *54*, 15347–15354. [CrossRef]

31. Yun, H.; Liang, B.; Ding, Y.; Li, S.; Wang, Z.; Khan, A.; Zhang, P.; Zhang, P.; Zhou, A.; Wang, A.; et al. Fate of antibiotic resistance genes during temperature-changed psychrophilic anaerobic digestion of municipal sludge. *Water Res.* **2021**, *194*, 116926. [CrossRef] [PubMed]

32. Vikromvarasiri, N.; Koyama, M.; Nakasaki, K.; Kurniawan, W.; Pisutpaisal, N. Enhancing methane recovery by intermittent substrate feeding and microbial community response in anaerobic digestion of glycerol. *Renew. Energy* **2023**, *204*, 106–113. [CrossRef]

33. Hussein, S.H.; Qurbani, K.; Ahmed, S.K.; Tawfeeq, W.; Hassan, M. Bioremediation of heavy metals in contaminated environments using Comamonas species: A narrative review. *Bioresour. Technol. Rep.* **2024**, *25*, 101711. [CrossRef]

34. Nittami, T.; Shoji, T.; Koshiba, Y.; Noguchi, M.; Oshiki, M.; Kuroda, M.; Kindaichi, T.; Fukuda, J.; Kurisu, F. Investigation of prospective factors that control Kouleothrix (Type 1851) filamentous bacterial abundance and their correlation with sludge settleability in full-scale wastewater treatment plants. *Process Saf. Environ. Prot.* **2019**, *124*, 137–142. [CrossRef]

35. Fan, Q.; Fan, X.; Fu, P.; Sun, Y.; Li, Y.; Long, S.; Guo, T.; Zheng, L.; Yang, K.; Hua, D. Microbial community evolution, interaction, and functional genes prediction during anaerobic digestion in the presence of refractory organics. *J. Environ. Chem. Eng.* **2022**, *10*, 107789. [CrossRef]

36. Liwarska-Bizukojć, E.; Olejnik, D. Activated sludge community and flocs morphology in response to aluminum oxide particles in the wastewater treatment system. *J. Water Process Eng.* **2020**, *38*, 101639. [CrossRef]

37. Rodrigues, C.V.; Camargo, F.P.; Lourenço, V.A.; Sakamoto, I.K.; Maintinguer, S.I.; Silva, E.L.; Varesche, M.B.A. Optimized conditions for methane production and energy valorization through co-digestion of solid and liquid wastes from coffee and beer industries using granular sludge and cattle manure. *J. Environ. Chem. Eng.* **2023**, *11*, 111250. [CrossRef]

38. Franchi, O.; Álvarez, M.I.; Pavissich, J.P.; Belmonte, M.; Pedrouso, A.; del Río, Á.V.; Mosquera-Corral, A.; Campos, J.L. Operational variables and microbial community dynamics affect granulation stability in continuous flow aerobic granular sludge reactors. *J. Water Process Eng.* **2024**, *59*, 104951. [CrossRef]

39. Qi, X.; Jia, X.; Wang, Y.; Xu, P.; Li, M.; Xi, B.; Zhao, Y.; Zhu, Y.; Meng, F.; Ye, M. Development of a rapid startup method of direct electron transfer-dominant methanogenic microbial electrosynthesis. *Bioresour. Technol.* **2022**, *358*, 127385. [CrossRef]

40. Ma, X.; Li, S.; Pan, R.; Wang, Z.; Li, J.; Zhang, X.; Azeem, M.; Yao, Y.; Xu, Z.; Pan, J.; et al. Effect of biochar on the mitigation of organic volatile fatty acid emission during aerobic biostabilization of biosolids and the underlying mechanism. *J. Clean. Prod.* **2023**, *390*, 136213. [CrossRef]